



Effects of Additives on Copper Electrodeposition in Submicrometer Trenches

Madoka Hasegawa, Yoshinori Negishi, Takuya Nakanishi, and Tetsuya Osaka^{*z}

Department of Applied Chemistry, School of Science and Engineering, Waseda University,
Tokyo 169-8555, Japan

Effects of the conventional bath additives [chloride ions (Cl^-), poly(ethylene glycol) (PEG), bis(3-sulfopropyl)disulfide (SPS), and Janus green B (JGB)] used in the damascene process on the filling of submicrometer trenches with electrodeposited copper were investigated by electrochemical polarization measurement and cross-sectional microscopy. The combination of Cl^- and PEG inhibited copper deposition in the areas of opening of the trenches, while SPS accelerated it at the bottom. Polarization curves showed that the degree of acceleration of copper deposition by SPS increases with the concentration of SPS. This SPS concentration-dependent acceleration accounts for the observed bottom-up growth. The addition of JGB inhibited copper deposition at the later stages of the filling process, leading to the suppression of the overfill phenomenon, although the bottom-up growth was also inhibited at high JGB concentrations. Bath agitation significantly enhanced the inhibition effect of JGB on the overfill phenomenon, without disturbing the bottom-up growth.

© 2005 The Electrochemical Society. [DOI: 10.1149/1.1867672] All rights reserved.

Manuscript submitted July 29, 2004; revised manuscript received October 16, 2004. Available electronically March 9, 2005.

Copper electrodeposition is used in the damascene process for the fabrication of interconnections of ultralarge-scale integrated semiconductor devices.¹ To accomplish “superfilling,” which means the void-free filling of trenches with electrodeposited copper, several additives such as chloride ions (Cl^-), poly(ethylene glycol) (PEG), bis(3-sulfopropyl)disulfide (SPS), and Janus green B (JGB) are included in the bath.²⁻⁴ Despite the successful use of the process in the semiconductor fabrication technology, the behavior of these additives during the copper electrodeposition process is still incompletely understood because of the complexity resulting from interactions between the effects of the multiple number of additives.²⁻⁵ Therefore, investigations for understanding additive effects on the copper electrodeposition inside submicrometer trenches have been carried out by many researchers.³⁻¹¹ It has been reported^{6,9,10} that “bottom-up” growth, in which the deposition from the bottom of trenches accelerated relative to that in the areas of openings of the trenches, occurred in the bath containing Cl^- , PEG, and SPS or its monomeric derivative. Many reports have shown that the addition of PEG with Cl^- inhibits copper deposition,^{3,6,12-18} whereas SPS accelerates the deposition when it is added together with PEG and Cl^- .^{19,20} It has been suggested that the competitive adsorption between the accelerator and the inhibitor results in the bottom-up effect.^{6,9,21-23} The bottom-up effect achieves the superfilling of copper in trenches, while it also brings about the “overfill” phenomenon, in which copper bumps are formed above the copper-filled trenches.^{3,6} Moffat *et al.*^{24,25} and West *et al.*⁹ have independently proposed models in which the coverage of accelerator at the bottom of trenches is assumed to increase during the filling of trenches. Their models predict not only the superfilling but also the “overfill” phenomenon, explaining successfully the fundamental aspects of the bottom-up growth. However, from a practical viewpoint, the overfill phenomenon itself is disadvantageous for the planarization step (chemical mechanical polishing, CMP), which follows the copper deposition in the damascene process. JGB is regarded to serve as a leveling agent, flattening these bumps of copper deposits on the surface,^{3,4} or to influence the filling properties.^{2,8} However, the behavior of JGB, particularly its interaction with other additives, is not well understood.

This paper discusses effects of Cl^- , PEG, SPS, and JGB on the filling of submicrometer trenches with electrodeposited copper based on both electrochemical polarization curves and practical observation of cross sections of trenches. We focused our attention in our study on the effect of JGB. To understand the effect of JGB on the overfill phenomenon caused by SPS, our investigation was car-

ried out successively for the bath containing Cl^- , PEG, and SPS (Cl-PEG-SPS bath), and the bath containing JGB as an additional component (Cl-PEG-SPS-JGB bath). Finally, an attempt was made to derive the mechanism for the inhibition of overfill phenomenon by JGB.

Experimental

The compositions of the baths used in this study are shown in Table I. The basic constituents of all baths used were 0.26 mol L⁻¹ CuSO_4 and 2.0 mol/L⁻¹ H_2SO_4 . Chloride ions (as HCl) and PEG, average molecular weight 2000, were added to make their concentrations equal to 50 and 100 ppm, respectively. The concentrations of SPS and JGB were varied, as indicated in Table I. All experiments were carried out at room temperature.

Polarization measurements were performed with a rotating disk electrode (RDE) system (RRDE-1, Nikko Keisoku) equipped with a computer-controlled electrochemical measuring system (HZ-3000, Hokuto Denko). A Cu disk working electrode (0.6 cm diam) was polished first with a no. 2000 emery paper and subsequently with 0.06 μm alumina paste on a sheet of polishing cloth. A Pt counter electrode and an Ag/AgCl reference electrode were used for the measurements. These electrodes were placed in a three-electrode cell. The RDE was rotated at a speed in a range of 0-2500 rpm. The measurements were performed at a potential scan rate of 2 mV s⁻¹. Before each experiment, the bath solution was deaerated by bubbling N_2 gas for 15 min.

For the trench-filling studies, substrates with trench arrays were employed. A Ta barrier layer and a Cu seed layer were sputtered onto an SiO_2/Si substrate. The trenches were 200 nm wide and 500 nm deep with an aspect ratio of 2.5. The space between the trenches was approximately equal to the trench width. The electrodeposition of copper was carried out galvanostatically at a current density of 10 mA cm⁻² using a paddle plating system (Uyemura) with or without agitation (100 rpm). The deposition time was varied from 15 to 90 s. After the electrodeposition, the specimen was cleaved perpendicularly to the direction of the trenches. The filling feature of copper in the trenches was examined by cross-sectional observation using a field-emission scanning electron microscope (S-4800, Hitachi).

Results

Polarization measurements.—Effect of Cl^- and PEG.—Figure 1 shows cathodic polarization curves for copper electrodeposition from the additive-free, PEG (Cl^- -free), and Cl-PEG baths. The polarization curve for the additive-free bath (Fig. 1a) shows that the current density gradually increased from the beginning of the potential scan and reached the plateau at about -0.4 V vs. Ag/AgCl. This

* Electrochemical Society Fellow.

^z E-mail: osakatet@waseda.jp

Table I. Bath compositions.

Bath name	CuSO ₄ (mol L ⁻¹)	H ₂ SO ₄ (mol L ⁻¹)	PEG (Mw 2000) (ppm)	Cl ⁻ (HCl) (ppm)	SPS (ppm)	JGB (ppm)
Additive-free	0.26	2.0				
PEG	0.26	2.0	100			
Cl-PEG	0.26	2.0	100	50		
Cl-PEG-SPS	0.26	2.0	100	50	1-1000	
Cl-PEG-SPS-JGB	0.26	2.0	100	50	1-5	1-50

plateau corresponds to the mass-transfer limiting current for the reduction of cupric ions at potentials more negative than -0.4 V. The continued negative scan beyond -0.6 V led to a significant increase in current density due to hydrogen evolution. The addition of PEG to the bath decreased the limiting current density (Fig. 1b). In the polarization curve for the Cl-PEG bath (Fig. 1c), the current was essentially nonexistent at potentials less negative than -0.1 V. As the shape and the limiting current density of the polarization curve for the Cl-PEG bath were identical to those for the PEG bath, it is seen that only the potential where the current began to increase was shifted in the negative direction by the addition of Cl⁻. This result suggests that the addition of both Cl⁻ and PEG greatly increased the overpotential for copper deposition, resulting in the inhibition of copper deposition.

To investigate the effect of mass transfer of these additives to the electrode, polarization measurements were performed at rotation speeds of 0, 100, and 2500 rpm with and without Cl⁻ and PEG (Fig. 2). In both cases, the current density increased with the rotation speed in the mass-transfer limited region, where the deposition rate of copper is controlled by the rate of diffusion of cupric ions. The limiting current densities on these cathodic polarization curves (insets of Fig. 2) varied linearly with $\omega^{1/2}$ as predicted by the Levich equation.²⁶ However, at potentials much less negative than those in the mass-transfer limited region, the current density was independent of the rotation speed.

Effect of SPS.—The polarization curves for the baths containing various concentrations of SPS together with Cl⁻ and PEG are shown in Fig. 3. The addition of SPS to the Cl-PEG bath brought about an increase in the slope of polarization curves, $\Delta i/\Delta E$, in the range of current density between -10 and -35 mA cm⁻², from ~ 0.3 to ~ 0.5 A cm⁻² V⁻¹, indicating that copper deposition is accelerated in the Cl-PEG-SPS bath (Fig. 4). Note that the slope $\Delta i/\Delta E$ was ~ 0.5 A cm⁻² V⁻¹ regardless of the SPS concentration in all polarization curves for the Cl-PEG-SPS baths. With an increase in SPS concentration, the potential where the current began to increase

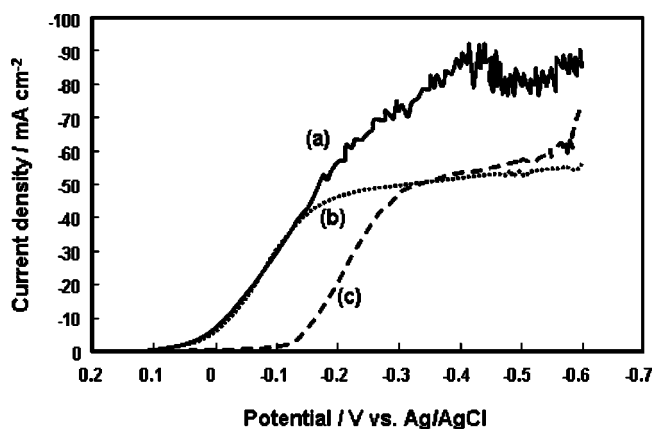


Figure 1. Cathodic polarization curves for copper electrodeposition from (a) additive-free, (b) PEG, and (c) Cl-PEG baths. Rotation speed of RDE and potential scan rate were 100 rpm and 2 mV s⁻¹, respectively.

shifted in the positive direction. Such a positive shift of potential is suggestive of the greater degree of acceleration of copper deposition at the higher SPS concentrations. However, at SPS concentrations higher than 1000 ppm, the dependence of the potential shift on SPS concentration was negligible, and the polarization curves were essentially identical to curve (e) in Fig. 3.

The rotation speed of the RDE affected the polarization characteristics for the Cl-PEG-SPS bath (Fig. 5) in practically the same manner as those for the additive-free and Cl-PEG baths shown in Fig. 2. The current density in the mass-transfer limited region (at potentials more negative than -0.16 V) increased with the rotation speed of RDE, as predicted by the Levich equation (inset of Fig. 5), whereas the current density was independent of the rotation speed at potentials less negative than -0.16 V.

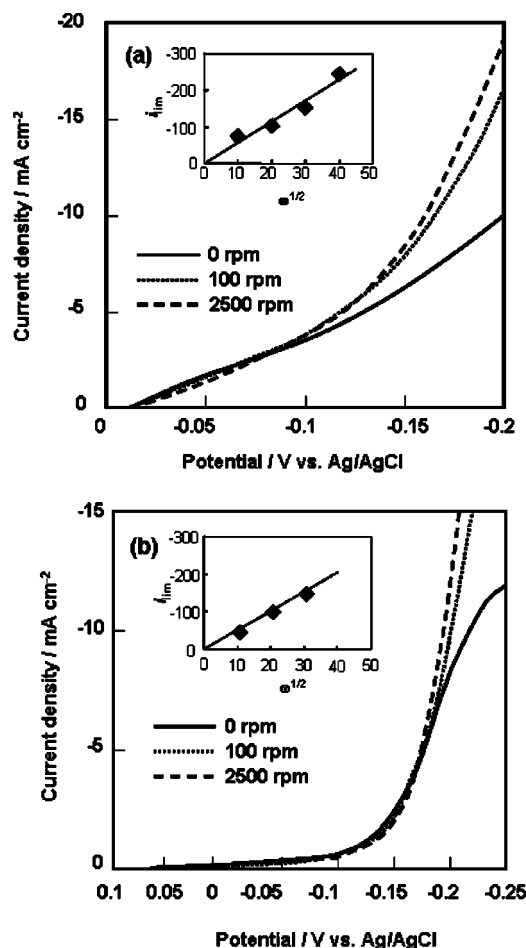


Figure 2. Dependence of polarization characteristics for copper electrodeposition from (a) additive-free and (b) Cl-PEG baths on the rotation speed of RDE. Rotation speeds of RDE were 0, 100, and 2500 rpm, and potential scan rate was 2 mV s⁻¹. Insets of (a) and (b) are Levich plots on limiting current density for additive-free and Cl-PEG baths, respectively.

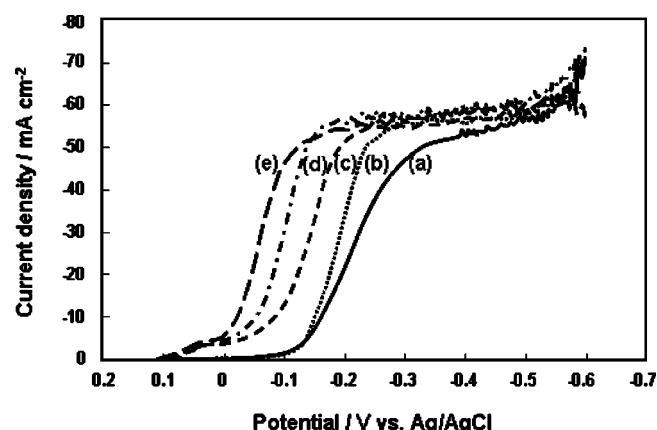


Figure 3. Effect of SPS concentration on polarization characteristics for copper electrodeposition from Cl-PEG-SPS baths containing (a) 0, (b) 1, (c) 10, (d) 100, and (e) 1000 ppm of SPS. Rotation speed of RDE and potential scan rate were 100 rpm and 2 mV s^{-1} , respectively.

Effect of JGB.—Polarization curves for the Cl-PEG-SPS-JGB baths containing various concentrations of JGB are shown in Fig. 6. The addition of JGB to the Cl-PEG-SPS bath resulted in a negative shift of the potential where the current density began to increase, which is in contrast to the effect of the addition of SPS to the Cl-PEG bath. The degree of the potential shift was greater at JGB concentrations higher than 10 ppm (Fig. 7). For the Cl-PEG-SPS-JGB bath, the current density in the mass-transfer limited region was not constant but fluctuated; nevertheless, it tended to be lower than that for the Cl-PEG-SPS bath. The potential shift in the polarization curves is attributable to the inhibition of copper deposition by JGB. The slope of the polarization curve, or $\Delta i/\Delta E$, was approximately equal to $0.5 \text{ A cm}^{-2} \text{ V}^{-1}$ at JGB concentrations between 0 and 10 ppm. The value increased to about $1.1 \text{ A cm}^{-2} \text{ V}^{-1}$ when 50 ppm of JGB was added.

The dependence of polarization characteristics for the Cl-PEG-SPS-JGB bath on the rotation speed is shown in Fig. 8. Note that the electrode rotation appears to suppress the cathodic reaction at potentials less negative than -0.17 V . This suppression was most significant at the rotation speed of 2500 rpm. At potentials more negative than -0.17 V , where copper deposition is controlled by the diffusion of cupric ions, the current density increased with the rotation speed of RDE (inset of Fig. 8).

Trench filling.—Effect of Cl^- and PEG.—Cross-sectional SEM images of trenches filled with electrodeposited copper from the additive-free and Cl-PEG baths are shown in Fig. 9. The deposition

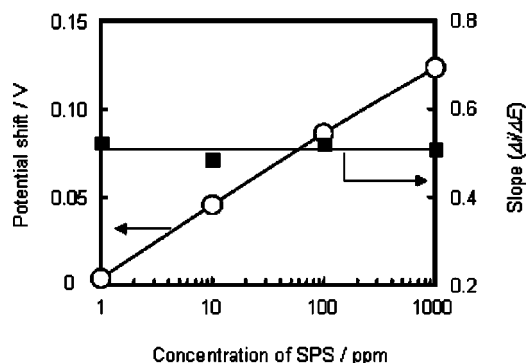


Figure 4. Plots of the shift of onset potential with respect to that for the SPS-free (Cl-PEG) bath and the slope of polarization curve ($\Delta i/\Delta E$; see text) against SPS concentration.

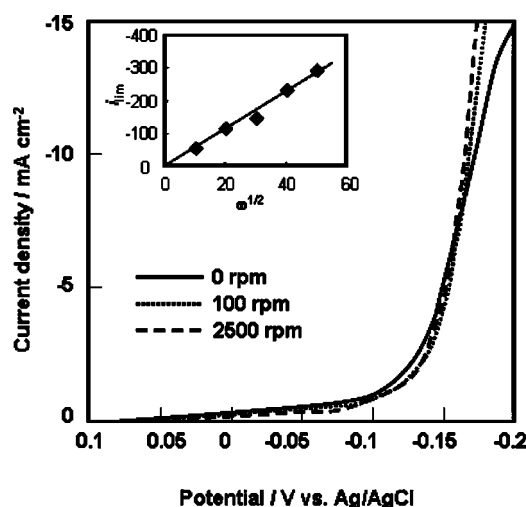


Figure 5. Dependence of polarization characteristics for copper electrodeposition from Cl-PEG-SPS bath on rotation speed of RDE. SPS concentration was 5 ppm. Rotation speeds of RDE were 0, 100, and 2500 rpm and the potential scan rate was 2 mV s^{-1} . Inset is a Levich plot on the limiting current density for the Cl-PEG-SPS baths.

was carried out under the static condition. The SEM images revealed the formation of voids in Cu-filled trenches. For the additive-free bath, the voids were spherical in shape (Fig. 9a). With the Cl-PEG bath, ellipsoidal voids with rough profiles were formed (Fig. 9b), while with the PEG (Cl^- -free) bath, voids formed in trenches were similar in shape to those formed with the additive-free bath (Fig. 9c).

To reveal the evolution with time of the filling feature of copper in trenches, the SEM observation of copper deposited in trenches was carried out with the deposition time as a variable (Fig. 10). The Cu deposition was performed without bath agitation. With the additive-free bath, a thick deposit of copper was observed at the edges of the openings of trenches in early stages of deposition process (Fig. 10a). The deposition proceeded, while maintaining the feature of bulge formation around the edges (Fig. 10b). Finally, the coalescence of round edges at the trench-openings resulted in void-formation in the Cu-filled trenches (Figs. 10c and d). On the other hand, with the Cl-PEG bath, conformal deposition was observed throughout the filling process. The sequential SEM images (Figs.

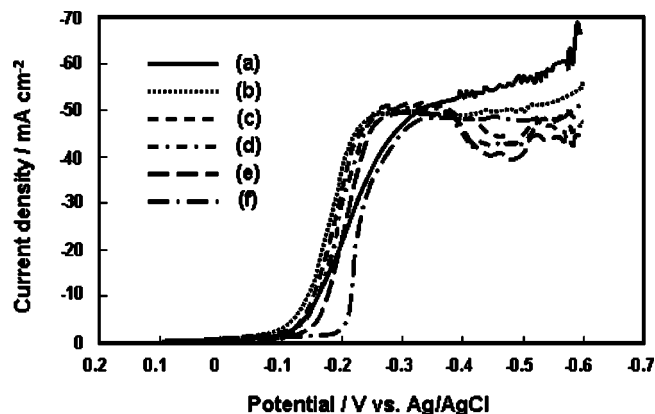


Figure 6. Effect of JGB concentration on polarization characteristics for copper electrodeposition. (a) Cl-PEG, (b) Cl-PEG-SPS, and (c–f) Cl-PEG-SPS-JGB baths containing (c) 1, (d) 5, (e) 10, and (f) 50 ppm of JGB. SPS concentration was 5 ppm. Rotation speed of RDE and potential scan rate were 100 rpm and 2 mV s^{-1} , respectively.

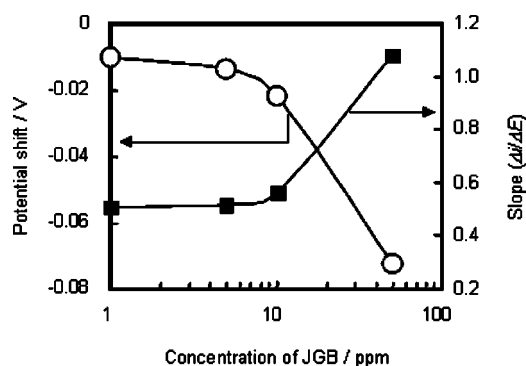


Figure 7. Plots of the shift of onset potential with respect to that for the JGB-free (Cl-PEG-SPS) bath and the slope of polarization curves ($\Delta i/\Delta E$; see text) against JGB concentration.

10e-h) show that the surface roughness of the merging sidewalls of trenches seems to form voids in the trenches at the later stages of the filling process (Figs. 10g and h).

To investigate the effect of mass transfer in the trenches, a series of trench-filling experiments was also carried out with bath agitation (SEM images not shown). With agitation, voids still formed in copper-filled trenches obtained from both the additive-free and the Cl-PEG baths. Evidently, agitation brought about no significant change in the filling feature for both baths.

Effect of SPS.—Figure 11 shows cross-sectional SEM images of trenches filled with copper from the Cl-PEG-SPS baths containing various concentrations of SPS. At SPS concentrations between 2 and 100 ppm, no voids were observed in Cu-filled trenches, although the thickness of copper deposits in the areas above trenches increased as compared with those obtained from the Cl-PEG bath. The increase in the thickness of copper deposits above trenches is considered to result from overlapping adjacent bumps. For wider trenches (SEM images not shown), the presence of bumps was apparent above each trench. This phenomenon, *i.e.*, an excessive deposition of copper above Cu-filled trenches, is known as the “overflow” phenomenon.^{3,6} The sequential SEM images (Fig. 12) revealed that the conformal deposition of copper proceeded during the first 30 s (Fig. 12a and b). At a deposition time of 60 s (Fig. 12c), the trenches were almost completely filled with copper, whereas the increase in copper thickness at the trench opening was relatively small. The results suggest

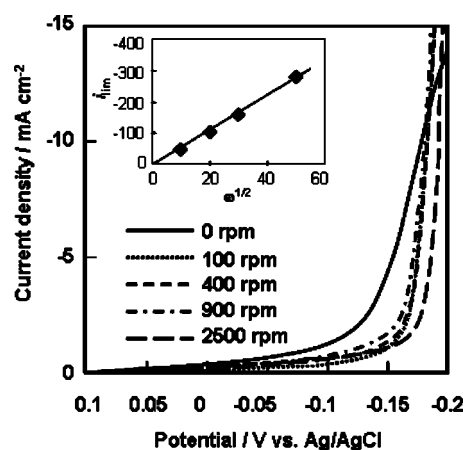


Figure 8. Dependence of polarization characteristics for the Cl-PEG-SPS-JGB bath on the rotation speed of RDE. Both SPS and JGB concentrations were 5 ppm. Rotation speeds of RDE were 0, 100, 400, 900, and 2500 rpm and potential scan rate was 2 mV s⁻¹. Inset is a Levich plot on the limiting current density for the Cl-PEG-SPS-JGB baths.

a greater degree of acceleration of copper deposition from the trench bottom compared with that from the sidewalls. These results for the Cl-PEG-SPS bath agreed with the previous results reported by Moffat *et al.*⁶ The overflow phenomenon became less significant with an increase in SPS concentration and disappeared completely with the addition of more than 500 ppm of SPS, which formed small defects in Cu-filled trenches (Fig. 11e). For the Cl-PEG-SPS baths, no significant effect of the agitation was observed, similarly to the results obtained with the additive-free and Cl-PEG baths.

Effect of JGB.—Furthermore, copper deposition in trenches from the baths containing various concentrations of JGB with Cl⁻, PEG, and SPS was investigated based on the cross-sectional SEM images (Fig. 13). With the addition of 1 and 2 ppm of JGB to the Cl-PEG-SPS bath, the thickness of copper deposits above Cu-filled trenches decreased, and the bumps above each trench became distinctive. The suppression of overflow phenomenon seems to decrease the bump overlapping. However, with the addition of 20 ppm of JGB, defects began to appear in the trenches although the overflow phenomenon was almost completely suppressed. The sequential SEM images (Fig. 14) showed that the conformal deposition proceeded during the

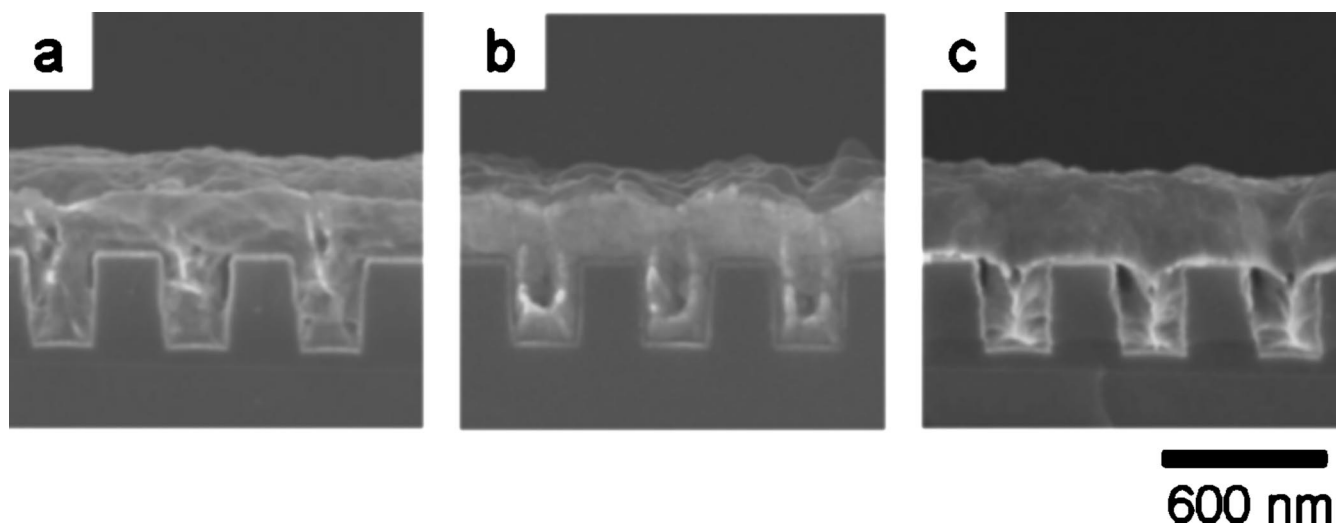


Figure 9. SEM images of copper electrodeposited in trenches from (a) additive-free, (b) Cl-PEG, and (c) PEG baths. Copper electrodeposition was performed galvanostatically at -10 mA cm^{-2} for 90 s without bath agitation.

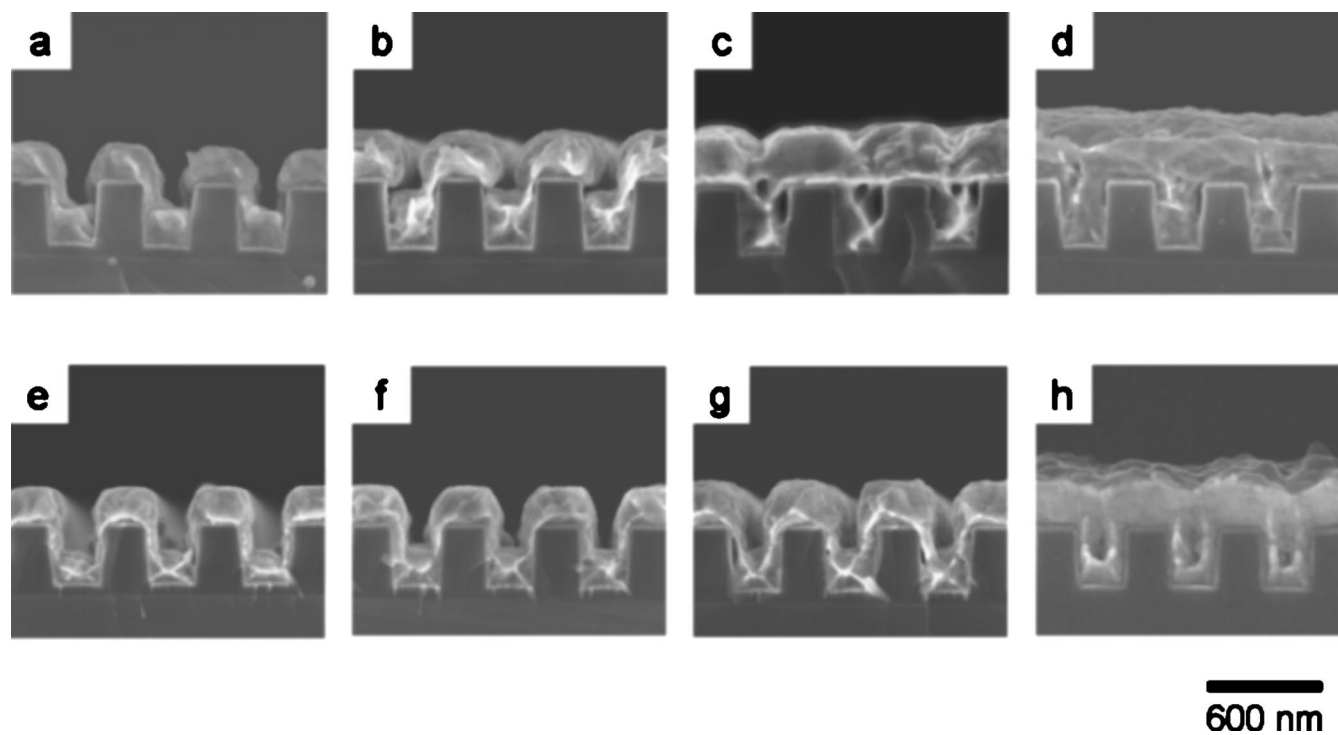


Figure 10. Cross-sectional SEM images of copper electrodeposited in trenches for filling sequences from (a–d) the additive-free and (e–h) Cl-PEG baths. Copper electrodeposition was performed galvanostatically at -10 mA cm^{-2} for 15, 30, 60, and 90 s (left to right) without bath agitation.

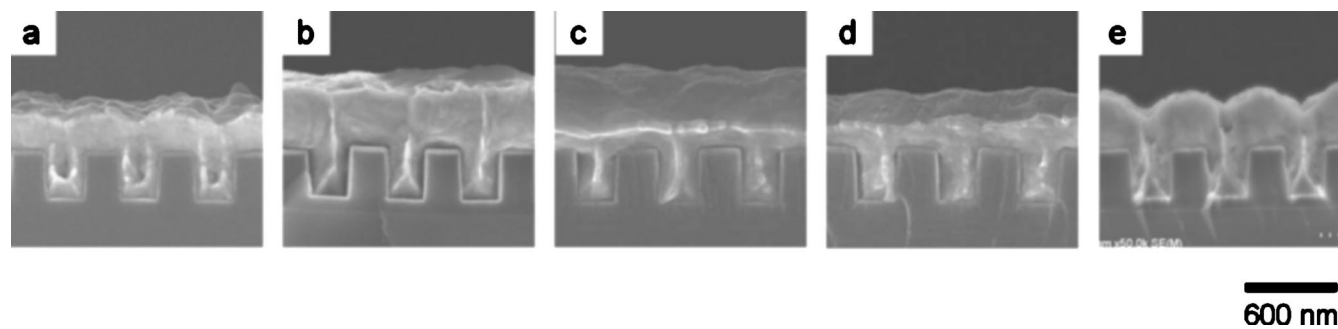


Figure 11. Cross-sectional SEM images of copper electrodeposited in trenches from the Cl-PEG-SPS baths. SPS concentrations were (a) 0, (b) 2, (c) 5, (d) 50, and (e) 500 ppm. Copper electrodeposition was performed galvanostatically at -10 mA cm^{-2} for 90 s without bath agitation.

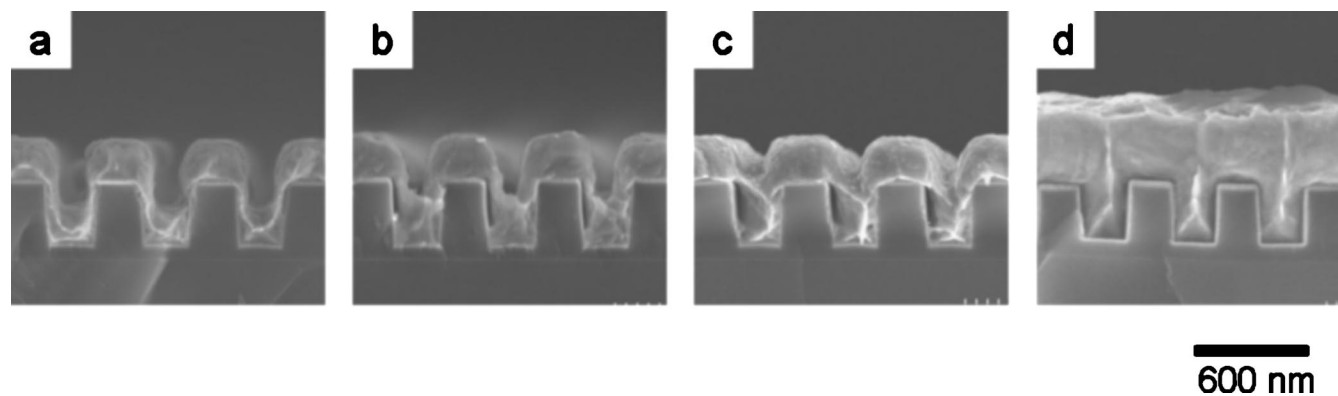


Figure 12. Cross-sectional SEM images of copper electrodeposited in trenches for filling sequences from the Cl-PEG-SPS bath. SPS concentration was 2 ppm. Copper electrodeposition was performed galvanostatically at -10 mA cm^{-2} for (a) 15, (b) 30, (c) 60, and (d) 90 s without bath agitation.

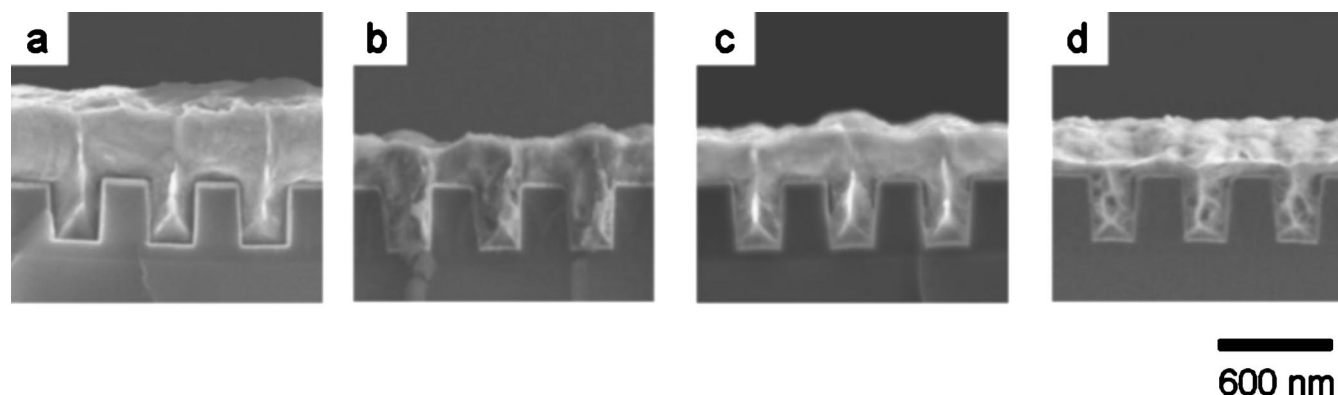


Figure 13. Cross-sectional SEM images of copper electrodeposited in trenches from the Cl-PEG-SPS-JGB bath. SPS concentration was 2 ppm, and JGB concentrations were (a) 0, (b) 1, (c) 2, and (d) 20 ppm. Copper electrodeposition was performed at -10 mA cm^{-2} for 90 s without bath agitation.

first 30 s, and that the accelerated deposition of copper from the bottom occurred at a deposition time of 60 s. During the first 60 s, the filling feature from the Cl-PEG-SPS-JGB bath was similar to that from the Cl-PEG-SPS bath. However, interestingly, the profile of deposits from the Cl-PEG-SPS-JGB bath was different from that formed in the Cl-PEG-SPS bath after 90 s of deposition. The thickness of copper deposits above Cu-filled trenches from the Cl-PEG-SPS-JGB bath was smaller than that from the Cl-PEG-SPS bath.

In contrast to the other baths, the effect of agitation was significant in the JGB-containing bath (Fig. 15). With agitation of the bath at a speed of 100 rpm, the bumps above trenches became much smaller, and a defect-free filling was obtained.

Discussion

Effect of Cl^- and PEG.—A significant inhibition of copper deposition at the openings of trenches was observed with baths containing Cl^- and PEG. As was discussed by Miura *et al.*,⁴ this inhibition seems to be related to the significant polarization observed in the polarization curve for the Cl-PEG bath (Fig. 1c). For the PEG bath (without Cl^-), the polarization curve (Fig. 1b) shows the suppression of the limiting current density without any shift of potential, as compared with the curve for the additive-free bath (Fig. 1a). As PEG is considered to adsorb onto the copper surface,^{12,16} the decrease in the limiting current density for the PEG bath appears to be due to adsorbed PEG molecules blocking the transport of cupric ions to the electrode surface. The strong inhibition of copper deposition observed with the Cl-PEG bath is suggested to result from the formation of a blocking layer consisting of the constituents of the

bath. It has been reported that PEG and Cl^- form a complex with cuprous or cupric ion.¹²⁻¹⁸ Yokoi *et al.*¹² reported that the blocking layer may consist of a complex of cuprous ion and PEG formed on specifically adsorbed chloride ions.

Effect of SPS.—The bottom-up growth in the presence of SPS was more distinct at lower concentrations of SPS, whereas it disappeared completely at high concentrations (Fig. 11). This SPS effect is accounted for by the acceleration of copper deposition by SPS observed in the polarization curves for the Cl-PEG-SPS baths. As shown in Fig. 3, the degree of acceleration of copper deposition increased with increasing SPS concentration, and it tended to saturate at high SPS concentrations. Figure 16 shows the relationship between SPS concentration and the current densities at -0.1 , -0.15 , and -0.2 V (vs. Ag/AgCl), where copper deposition proceeded in trenches. In the range of low concentrations of SPS, the current density increased with increasing SPS concentration, indicating strong dependence of the copper deposition rate on SPS concentration. However, the slope of the current density vs. concentration curves becomes smaller at higher concentrations of SPS, suggesting that the concentration dependence of the degree of acceleration in this concentration range is small.

This SPS concentration-dependent acceleration accounts for the observed difference in the mode of trench filling at different SPS concentrations shown in Fig. 11. These experimental results can be explained by the mechanism of the bottom-up growth proposed by Moffat *et al.*^{24,25} In their model, SPS is accumulated at the bottom of trenches because of the decrease in surface area at the bottom during the trench-filling process. SPS is assumed to remain at the copper-

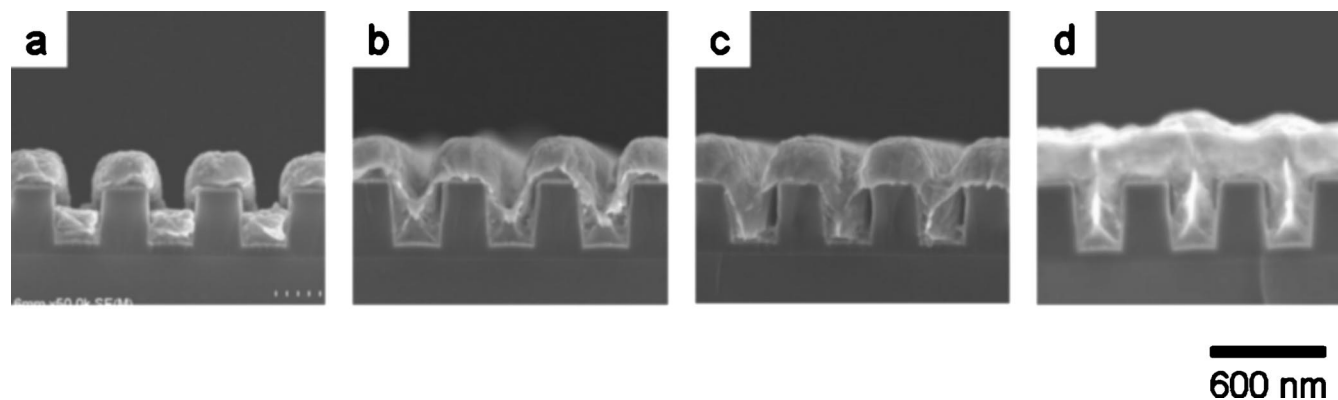


Figure 14. Cross-sectional SEM images of copper electrodeposited in trenches for filling sequences from the Cl-PEG-SPS-JGB baths. Both SPS and JGB concentrations were 2 ppm. Copper electrodeposition was performed galvanostatically at -10 mA cm^{-2} for (a) 15, (b) 30, (c) 60, and (d) 90 s without bath agitation.

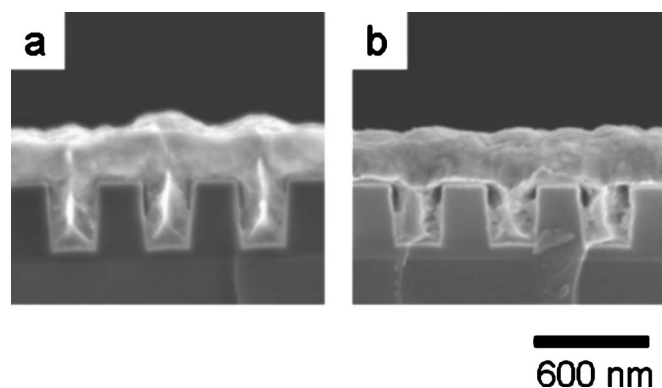


Figure 15. Cross-sectional SEM images of copper deposited in trenches from the Cl-PEG-SPS-JGB bath with agitation of the bath. Both SPS and JGB concentrations were 2 ppm. Agitation speeds were (a) 0 and (b) 100 rpm.

electrolyte interface during copper deposition without being consumed. This accumulation of SPS at the bottom is considered to result in the bottom-up growth. Based on this model, the dependence of the growth mode on SPS concentration shown in Fig. 11 can be interpreted as follows. At low concentrations of SPS, the deposition rate of copper strongly depends on SPS concentration. Therefore, the “coverage gradient” (surface concentration gradient) of SPS along the trench wall provides a significant difference in deposition rate at the bottom and at the top of the trench. In contrast, with excess SPS, the acceleration of copper deposition is saturated. In this case, the degree of acceleration of copper deposition is also the same at all locations on the trench wall. The constant acceleration of copper deposition brings about the conformal growth of copper in trenches, which leaves defects in copper-filled trenches.

Effect of JGB.—Haba *et al.*⁸ investigated the effect of JGB in the damascene copper electrodeposition without adding SPS. According to their report, the addition of JGB without SPS also achieves bottom-up filling when there is a suitable concentration gradient of JGB generated in a trench from the balance between the diffusion rate and the consumption rate of JGB.

In this study, as JGB was added with SPS, the bottom-up growth was brought about mainly by SPS, and the effect of JGB on the filling process appeared to be insignificant. The cross-sectional SEM images show that the inhibition of the “overflow” phenomenon occurs at the later stages of the copper-filling process, and it is enhanced by an increase in JGB concentration (Fig. 13 and 14). The inhibition of the overflow phenomenon and its dependence on JGB concentration are related to the shift of polarization curves in the negative direction brought about by the addition of JGB (Fig. 7). This negative shift is indicative of inhibition of copper deposition by JGB. The JGB effect appearing only at the later stages of trench-filling is considered to be relevant to the depletion of JGB within the trenches. In contrast to the effect of SPS (described in the preceding section), JGB is reported to be consumed on the copper surface during the copper deposition.⁸ Thus, within the trenches, where the supply of additives from the bulk of the solution is retarded as compared with the outside of the trenches, the consumption of JGB should lead to a decrease in JGB concentration. Although the inhibition became greater at higher concentrations of JGB, not only the overflow phenomenon but also the bottom-up growth was inhibited at high concentrations of JGB.

Note here that the effect of agitation of the bath was noticeable only for the Cl-PEG-SPS-JGB bath. Of particular interest is that agitation was effective for the inhibition of the overflow phenomenon, while little effect was observed for the bottom-up growth of copper in trenches (Fig. 15). The agitation effect observed in the SEM images should be attributable to the enhanced transfer of JGB to the electrode surface, in view of the results that no influence of agitation

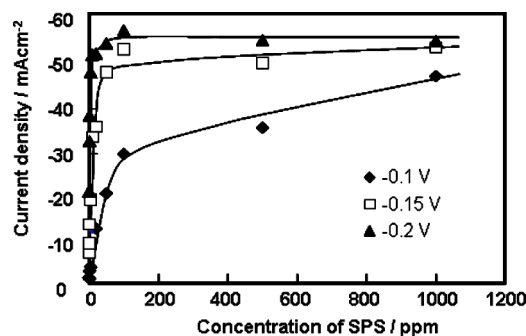


Figure 16. Dependence of current densities on SPS concentration at (◆) -0.1 , (□) -0.15 , and (▲) -0.2 V vs. Ag/AgCl.

on the filling feature of copper was observed for the other JGB-free baths. The results of polarization measurements performed at various rotation speeds of the RDE (Fig. 2, 5, and 8) also support this interpretation. The effect of RDE rotation speed on polarization characteristics at potentials less negative than that of the mass-transfer limited region was significant only for the Cl-PEG-SPS-JGB bath, although the limiting current densities satisfied the Levich relation for all baths. The polarization curves for the Cl-PEG-SPS-JGB baths recorded with the rotation of the RDE shifted in the more negative direction compared with the polarization curve obtained in the static bath. This negative shift is considered to be due to the enhancement of the inhibition of copper deposition with an increase in mass transfer of JGB molecules to the electrode surface. These results suggest that the transfer of JGB molecules influences the copper deposition rate, unlike that of the other additives. Because agitation is considered to affect insignificantly the fluid flow within submicrometer trenches,²⁷ the enhancement of JGB transfer by agitation is assumed to be insignificant within trenches compared with the outside of the trenches. Thus, the significant enhancement of JGB transfer at the outside of trenches by agitation of the bath is expected to bring about a strong inhibition of the overflow phenomenon without inhibiting the bottom-up growth.

Conclusion

Superfilling of copper in submicrometer trenches from the Cl-PEG-SPS-JGB bath was investigated from both polarization curves and microscopic observation of trench filling. The mechanism of superfilling in the system of the Cl-PEG-SPS-JGB bath was discussed, particularly with a focus on the inhibition of overflow phenomenon by JGB. Copper electrodeposition at the opening of the trenches is inhibited by the combination of Cl^- and PEG throughout the deposition process. Bottom-up growth occurred in the presence of SPS and was considered to be relevant to the SPS concentration-dependent acceleration of copper deposition observed in polarization curves. JGB inhibits the overflow phenomenon in the later stages of the deposition process. However, a high concentration of JGB inhibited the bottom-up growth, which resulted in void formation. Bath agitation inhibited the overflow phenomenon significantly without producing voids in copper-filled trenches. The effect of agitation is considered to result from the enhanced transfer of JGB at the exterior of trenches. Therefore, the mass-transfer dependent inhibition by JGB is especially important for achieving bottom-up growth with suppression of the overflow phenomenon.

Acknowledgments

This work was carried out under the 21st Century Center of Excellence (COE) program Center for Practical Nano-Chemistry. This work was supported by Grant-in-Aid for COE Research, Molecular Nano-Engineering, from the Ministry of Education, Culture, Sports, Science and Technology, Japan. The authors thank Dr. Tokihiko Yokoshima for the discussion. T.N. acknowledges the Research Fellowship of the Japan Society for the Promotion of Science for

Young Scientists. The assistance in manuscript preparation provided by Dr. Yutaka Okinaka is gratefully acknowledged.

Waseda University assisted in meeting the publication costs of this article.

References

1. P. C. Andricacos, C. Uzoh, J. O. Dukovic, J. Horkans, and H. Deligianni, *IBM J. Res. Dev.*, **42**, 567 (1998).
2. J. J. Kelly and A. C. West, *Electrochem. Solid-State Lett.*, **2**, 561 (1999).
3. P. Taepaisitphongse, Y. Cao, and A. C. West, *J. Electrochem. Soc.*, **148**, C492 (2001).
4. S. Miura, K. Oyamada, Y. Takada, and H. Honma, *Electrochemistry (Tokyo, Jpn.)*, **69**, 773 (2001).
5. M. Kang and A. A. Gewirth, *J. Electrochem. Soc.*, **150**, C426 (2003).
6. T. P. Moffat, J. E. Bonevich, W. H. Huber, A. Stanishevsky, D. R. Kelly, G. R. Stafford, and D. Josell, *J. Electrochem. Soc.*, **147**, 4524 (2000).
7. T. P. Moffat, D. Wheeler, C. Witt, and D. Josell, *Electrochem. Solid-State Lett.*, **5**, C110 (2002).
8. T. Haba, T. Itabashi, H. Akahoshi, A. Sano, K. Kobayashi, and H. Miyazaki, *Mater. Trans., JIM*, **43**, 1593 (2002).
9. A. C. West, S. Mayer, and J. Reid, *Electrochem. Solid-State Lett.*, **4**, C50 (2001).
10. D. Josell, B. Baker, C. Witt, D. Wheeler, and T. P. Moffat, *J. Electrochem. Soc.*, **149**, C637 (2002).
11. M. Kang, M. E. Gross, and A. A. Gewirth, *J. Electrochem. Soc.*, **150**, C292 (2003).
12. M. Yokoi, S. Konishi, and T. Hayashi, *Denki Kagaku oyobi Kogyo Butsuri Kagaku*, **52**, 218 (1984).
13. D. Stoychev and C. Tsvetanov, *J. Appl. Electrochem.*, **26**, 741 (1996).
14. J. J. Kelly and A. C. West, *J. Electrochem. Soc.*, **145**, 3472 (1998).
15. J. J. Kelly and A. C. West, *J. Electrochem. Soc.*, **145**, 3477 (1998).
16. J. P. Healy, D. Pletcher, and M. Goodenough, *J. Electroanal. Chem. Interfacial Electrochem.*, **338**, 155 (1992).
17. V. D. Jovic and B. M. Jovic, *J. Serb. Chem. Soc.*, **66**, 935 (2001).
18. Z. V. Feng, X. Li, and A. A. Gewirth, *J. Phys. Chem. B*, **107**, 9415 (2003).
19. M. Tan and J. N. Harb, *J. Electrochem. Soc.*, **150**, C420 (2003).
20. J. J. Kim, S.-K. Kim, and Y. S. Kim, *J. Electroanal. Chem.*, **542**, 61 (2003).
21. Y. Cao, P. Taepaisitphongse, R. Chalupa, and A. C. West, *J. Electrochem. Soc.*, **148**, C466 (2001).
22. K. Kondo, N. Yamakawa, Z. Tanaka, and K. Hayashi, *J. Electroanal. Chem.*, **559**, 137 (2003).
23. K. Kondo, T. Matsumoto, and K. Watanabe, *J. Electrochem. Soc.*, **151**, C250 (2004).
24. T. P. Moffat, D. Wheeler, W. H. Huber, and D. Josell, *Electrochem. Solid-State Lett.*, **4**, C26 (2001).
25. D. Josell, D. Wheeler, W. H. Huber, and T. P. Moffat, *Phys. Rev. Lett.*, **87**, 016102 (2001).
26. A. J. Bard and L. R. Faulkner, *Electrochemical Methods*, p. 288, John Wiley & Sons, New York (1980).
27. K. M. Takahashi and M. E. Gross, *J. Electrochem. Soc.*, **146**, 4499 (1999).